Quaternary Research

doi:10.1017/qua.2020.50

THEMATIC SET
SHEMAX

Vegetation over the last glacial maximum at Girraween Lagoon, monsoonal northern Australia

Cassandra Rowe[a]*, Christopher M. Wurster[a], Costijn Zwart[a], Michael Brand[a], Lindsay B. Hutley[b], Vladimir Levchenko[c], Michael I. Bird[a]

[a]College of Science and Engineering, ARC Centre of Excellence of Australian Biodiversity and Heritage and Centre for Tropical Environmental and Sustainability Science, James Cook University, Cairns, QLD 4870, Australia
[b]Research Institute for the Environment and Livelihoods, Charles Darwin University, Darwin, Northern Territory 0909, Australia
[c]Australian Nuclear Science and Technology Organization, Locked Bag 2001, Kirrawee DC NSW 2232, Australia
*Corresponding author at: cassandra.rowe@jcu.edu.au (C. Rowe)

(Received January 13, 2020; Accepted May 5, 2020)

Abstract

Northern Australia is a region where limited information exists on environments at the last glacial maximum (LGM). Girraween Lagoon is located on the central northern coast of Australia and is a site representative of regional tropical savanna woodlands. Girraween Lagoon remained a perennial waterbody throughout the LGM, and as a result retains a complete proxy record of last-glacial climate, vegetation and fire. This study combines independent palynological and geochemical analyses to demonstrate a dramatic reduction in both tree cover and woody richness, and an expansion of grassland, relative to current vegetation at the site. The process of tree decline was primarily controlled by the cool-dry glacial climate and CO_2 effects, though more localised site characteristics restricted wetland-associated vegetation. Fire processes played less of a role in determining vegetation than during the Holocene and modern day, with reduced fire activity consistent with significantly lower biomass available to burn. Girraween Lagoon's unique and detailed palaeoecological record provides the opportunity to explore and assess modelling studies of vegetation distribution during the LGM, particularly where a number of different global vegetation and/or climate simulations are inconsistent for northern Australia, and at a range of resolutions.

Keywords: Tropical savanna; Grassland; Tree cover; Pollen; Charcoal; Carbon isotope; Model; Monsoon; Last Glacial Maximum; Northern Australia

INTRODUCTION

The last glacial maximum (LGM; centred on 21 ka) was the most recent time when ice sheets were at their maximum extent and hence sea level was at its lowest (Clark et al., 2009; Hopcroft and Valdes, 2015). Lowered sea level led to dramatic increases in land area in some parts of the world. Equally dramatic changes in the distribution of terrestrial biomes were driven by decreases in temperature, changes in the distribution and amount of precipitation, and lower atmospheric CO_2 (Ganopolski et al., 1998; Shakun and Carlson, 2010; Alder and Hostetler, 2015; Jiang et al., 2015).

Mapping regional changes in palaeogeography and climate at the LGM through the development of palaeoenvironmental proxy records from around the world is key to understanding modern patterns of biodiversity (Weigelt et al., 2016; Blonder et al., 2018; Ye et al., 2019) as well as the timing and trajectory of human dispersal (Gavashelishvili and Tarkhnishvili, 2016; Vahdati et al., 2019) and adaptation (Williams et al., 2018). The mapping of biome distributions at the LGM also provides empirical insight into climate at the LGM and therefore the opportunity to evaluate the reliability of climate and carbon/water models in reproducing observations from outside the comparatively small range of recent observed climate variability (Harrison et al., 2015).

Computer simulations, now Dynamic Global Vegetation Models (DGVMs), have long been used to simulate biome distributions in the present (Prentice et al., 1992) and at the LGM (Harrison and Prentice, 2003). The spatial distribution of vegetation types is driven by one or more general circulation models (GCMs), more recently incorporating other factors including plant responses to CO_2 (e.g., Cleator et al., 2019), fire regime (e.g., Calvo and Prentice., 2015; Scheiter et al., 2015) and herbivore biomass (Zhu et al., 2018). Simulations are tested against observations derived from well-

Cite this article: Rowe, C., Wurster, C. M., Zwart, C., Brand, M., Hutley, L. B., Levchenko, V., Bird, M. I. 2021. Vegetation over the last glacial maximum at Girraween Lagoon, monsoonal northern Australia. *Quaternary Research* 102, 39–52. https://doi.org/10.1017/qua.2020.50

dated proxy records, mostly commonly palynological investigations (Bartlein et al., 2011; Harrison et al., 2015).

The spatial distribution of observations of vegetation at the LGM (here defined as 21 ± 2 ka; Hopcroft and Valdes, 2015) is clearly critical to achieving an observation-informed representation of biome distribution at the LGM. Observations of sufficient quality for this purpose are currently weighted heavily toward studies from the higher latitudes, with much patchier representation of low latitude areas (Bartlein et al., 2011; Cleator et al., 2019). This in turn means that observations provide no empirical constraints on vegetation for large parts of the terrestrial biosphere, with those in the southern hemisphere biosphere particularly poor (Cleator et al., 2019).

Northern Australia is one region where there is limited information on vegetation distribution at the LGM (Pickett et al., 2004), with the only sites in the global database of Bartlein et al. (2011) located on the northeast coast—a wet, mountainous, tropical forest covered region that is atypical of the rest of tropical Australia. At the LGM, lowered sea level (Yokoyama et al., 2019) meant that much of the modern landmass of northern Australia was ~300 km inland of the LGM coast (Williams et al., 2018). Currently, the equivalent distance inland reduces mean annual precipitation from 1700 mm to approximately1000 mm. This rainfall gradient inland from the coast, along with potential changes in monsoon strength at the LGM (Jiang et al., 2015; Denniston et al., 2017; Yan et al., 2018) means northern Australia is sensitively placed to provide a meaningful test of DGVM skill using LGM boundary conditions. Recent modelling studies of vegetation distribution during the LGM using a number of different DGVMs and GCMs, at a range of resolutions, have not converged on a common result for the northern Australian region, with simulations broadly characterizable as ranging from grassland through savanna woodland to tropical forest (Calvo and Prentice, 2015; Gavashelishvili and Tarkhnishvili, 2016; Zhu et al., 2018; Lu et al., 2019; Chen et al., 2019; Dallmeyer et al., 2019).

Here we present a detailed palynological investigation of the LGM from Girraween Lagoon near Darwin, on the central northern coast of Australia. This site is representative of the lowland tropical savanna-woodlands of northern Australia, at the southern end of the Indonesian-Australian Summer Monsoon (IASM) region. Scheiter et al. (2015) have demonstrated that Australian tropical savannas are currently sensitive to both climate change and fire management. It is the primary purpose of this paper to provide a detailed assessment of the response of vegetation to LGM environmental conditions at a location representative of the tropical savannas that currently cover approximately 20% of Australia's landmass.

STUDY AREA AND METHODS

Study area

Girraween Lagoon is one of a number of lagoons that occur across the Northern Territory's (NT's) Darwin region (Fig. 1). The site is located within the Howard River subcatchment of Darwin Harbour (12.517°S, 131.081°E; 28 km inland from the harbour's northern shoreline and tidal estuaries 15 km west; Schult, 2004). An extensive overview of the regional context has been provided by Rowe et al. (2019a) and only a brief description is given here.

The Köppen-Geiger classification (as redefined by Peel et al., 2007) characterises the northern NT climate as Tropical Savanna (code Aw). A distinctive feature of this region's climate is strong rainfall seasonality, driven by the annual north-

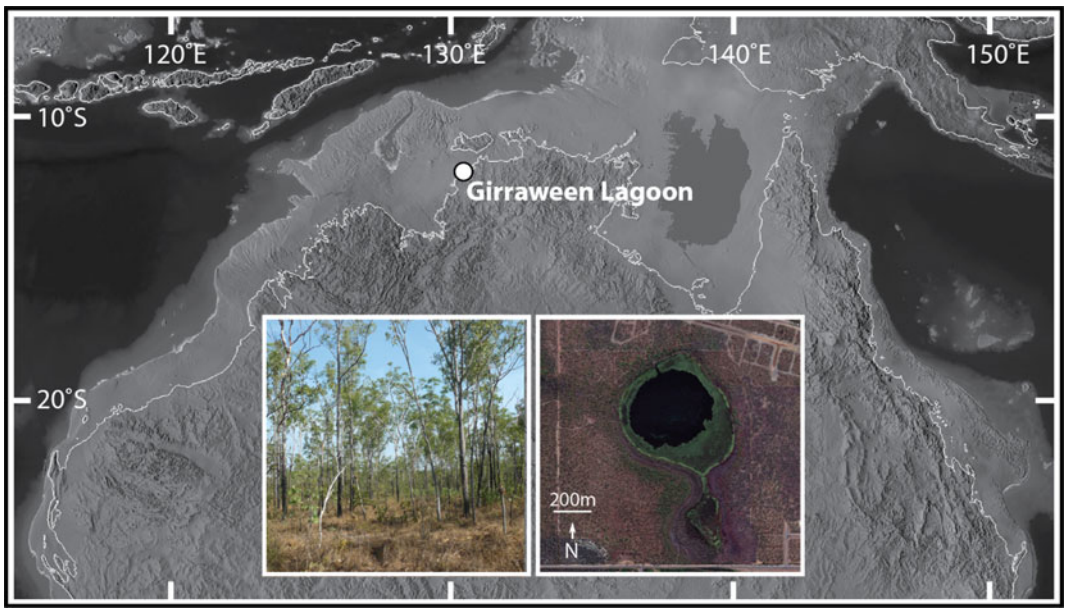

Figure 1. (color online) Location of Girraween Lagoon with current coastline mapped onto the landmass of Sahul, exposed by sea-level fall at the LGM. The outline of Sahul shown at a sea level equivalent to the 120 m isobath. Inset is a satellite image of the site and an image of the current dryland vegetation around the site.

https://doi.org/10.1017/qua.2020.50 Published online by Cambridge University Press

south migrating Intertropical Convergence Zone (ITCZ) with associated convective activity and extreme weather events such as tropical cyclones. El Niño–Southern Oscillation (ENSO) is currently an important driver in inter-annual variations in rainfall of the region (Charles et al., 2016). Mean annual Darwin rainfall is 1731.2 mm, and approximately 95% of this total falls during the wet-season months (November–April). Darwin experiences uniformly high temperatures; mean monthly maximum-minimum temperatures are 32.1°C and 23.2°C, respectively. Evaporation is also high year-round, but exhibits a strong seasonal pattern, ranging from ca. 200 mm per month during the October wet season build-up to ca.125 mm per month during the middle (June) of the dry season (Charles et al., 2016; Bureau of Meteorology, 2019, Darwin Airport, station 014015, 1941–2018).

Girraween Lagoon is a perennial fresh waterbody, with a surface area of 45 hectares (ha) and a maximum depth of 5 m. Water drains into the lagoon from a catchment of 917 ha. The lagoon is immediately underlain by lateritized and heavily weathered sandy to clayey Cretaceous sediments (30–50 m depth). These sediments are underlain by a Proterozoic dolomite aquifer. The lagoon originated as sinkhole due to collapse into voids created by dissolution of this underlying dolomite (McFarlane et al., 1995).

Modern catchment vegetation comprises tropical mesic open-forest savanna and/or savanna woodland (Hutley et al., 2013; Moore et al., 2016). *Eucalyptus tetrodonta*, *E. miniata*, and *Corymbia polycarpa* (all Eucalypteae: Myrtaceae) dominate the overstorey. Other prominent tree species include *Erythrophleum chlorostachys* (Caesalpinioideae: Fabaceae), *Lophostemon lactifluus* (Lophostemoneae: Myrtaceae) and *Terminalia ferdinandiana* (Combretaceae). In the understorey, *Sorghum* and *Heteropogon* (Poaceae) species are abundant. Saplings, shrubs (e.g., *Pandanus* [Pandanaceae], *Grevillea* [Proteaceae], *Calytrix* [Chamelaucieae: Myrtaceae] and broadleaf herbs (e.g., *Spermacoce* [Rubiaceae], *Murdannia* [Commelinaceae)], *Flagellaria* [Flagellariaceae]) vary in density and height, dependent on seasonal rainfall variation and fire history. Variable transitional plant communities occur on approach to the water, including mixed monsoonal and/or riparian forest associations; see Web and Tracey (1994) for discussion on monsoon-type drier rainforests, and Brock (1995) for survey results on Darwin remnant mixed species woodland. *Melaleuca symphyocarpa*, *M. viridiflora* and/or *M. cajuputi* (Melaleuceae: Myrtaceae) along with Cyperaceae-dominated sedgeland, form a swamp fringe around open water. Aquatic plants include *Nymphaea hastifolia* and *N. violacea* (Nymphaeaceae) as well as submergents such as *Najas* (Hydrocharitaceae). Girraween's catchment has burnt ≤ 6–7 times since the year 2000, equating to a fire return interval of 2–3 years, a typical regime of northern NT savanna (Russell-Smith and Yates, 2007).

The Larrakia Nation maintains Darwin regional traditional customary associations with Country, including within the Howard River area and Girraween Lagoon catchment (Burns 1999; Wells, 2001). Wells (2001) provides an account of Darwin history from a Larrakia perspective.

Methods

Girraween Lagoon was cored using a floating platform with hydraulic coring-rig. A 19.4 m core in 1 m sections was collected to the point of bedrock. The focus of this paper is the 478–598 cm section encompassing the LGM as well as the interval immediately before and after the LGM. Details and imagery of field, laboratory and microscope methods are reported in Rowe et al. (2019a, 2019b).

Pollen and charcoal analysis

Two cubic centimeter sediment samples were processed for pollen and microcharcoal analysis. Sample preparation followed the techniques as detailed in Rowe et al. (2019a, 2019b; see also references used therein). Chemical preparations (including $Na_4P_2O_7$, KOH, HCl, acetolysis and C_2H_5OH washes) were selected to initially disperse the organic-mineral matrix then progressively remove humic acids, calcium carbonates, bulk (in)organics, and silicates, as well as to render pollen ornamentations visible. Sieving took place at 7 µm and 125 µm. A *Lycopodium* spike (Lunds University batch 3862) was added during laboratory preparations, to determine concentrations of pollen and microcharcoal particles. Final residues were mounted in glycerol. Pollen counts are a minimum of 150 grains (including spores) per sample (single sample exception identified and described below). Pollen identification was based upon regionally representative floral reference libraries in development by the lead author (CR), and on online resources including the Australasian Pollen and Spore Atlas (http://apsa.anu.edu.au/). For additional information on Myrtaceae pollen identification, refer to Stevenson et al. (2015).

Insight into plant ecologies was gained through sources such as FloraNT (eflora.nt.gov.au). All data were plotted using TGView (Grimm, 2004). A dendrogram produced by CONISS (Grimm, 1987; 2004) was used to help in selection of diagram zone boundary location. Pollen was divided into eight groups to capture plant form and/or vegetation type. These groups were then classified further and allocated into plant-function and/or environmental response categories: dryland and wetland associated Myrtaceae, other woody taxa (sclerophyll or monsoonal forest affiliated), Poaceae, herbaceous taxa, pteridophtes and wetland associates (plant terms 'wetland' and 'aquatic' are used in reference to areas of seasonal verses permanent inundation, respectfully). These groups were then condensed further, and pollen allocated into plant-function and/or environmental response categories. Such categories helped evaluate fire tolerances as well as assess wet–dry continuums. Rowe et al. (2019a) provide an extended discussion on the allocation and use of plant functional types for the Girraween pollen record. All pollen types are identified to the most refined taxonomic level possible. In certain cases (e.g., Fabaceae, Myrtaceae) grain morphological descriptors are included in the categorisations to help highlight differing grain types. Accounting for pollen types in this way ensures diversity within the record is not

https://doi.org/10.1017/qua.2020.50 Published online by Cambridge University Press

lost. Microcharcoal particles (black, opaque, angular, >10 µm in length) were counted simultaneously with pollen and as an indicator of landscape fire Charcoal, as a proxy for local to regional fire occurrence, is guided by the advice of Whitlock and Larsen (2002) and as used in Rowe et al. (2019a).

Hydrogen pyrolysis of stable polycyclic aromatic carbon

Fifteen samples from a subset of depth intervals were analysed for the abundance and carbon isotope composition of total organic carbon (TOC) and pyrogenic carbon (PyC), by hydrogen pyrolysis (HyPy). HyPy quantifies PyC present as stable polycyclic aromatic carbon (SPAC) which has been shown to comprise compounds of more than seven condensed polycyclic aromatic rings (Meredith et al., 2012; Wurster et al., 2012, 2013). The technique has been described in detail in a number of publications (e.g., Ascough et al., 2009; Meredith et al., 2012). Briefly, 25–100 mg aliquots of each sample were loaded with a molybdenum (Mo) catalyst using an aqueous/methanol (1:1) solution of ammonium dioxydithiomolybdate $[(NH_4)_2MoO_2S_2]$. Catalyst weight was ~10% sample weight for all samples to give a nominal loading of 1% Mo. After sample loading, the reactor was pressurized with hydrogen to 15 GPa with a sweep gas flow of 5 L min^{-1}, then heated using a pre-programmed temperature profile, where samples are initially heated at a rate of 300°C min^{-1} to 250°C, then heated at a rate of 8°C min^{-1} until the final hold temperature of 550°C for 5 min.

Carbon abundance and isotope composition of samples were determined using a Costech Elemental Analyzer fitted with a zero-blank autosampler coupled via a ConFlow 4010 to a ThermoFinnigan DeltaV^{PLUS} using Continuous-Flow Isotope Ratio Mass Spectrometry (CF-IRMS) at the Advanced Analytical Unit at James Cook University, Cairns. Stable isotope results are reported as per mil (‰) deviations from the Vienna Pee Dee Belemnite (VPDB) reference standard scale for $\delta^{13}C$ values. Precisions (σ) on internal standards were better than ± 0.1‰.

Radiocarbon dating and age model development

Four samples of bulk sediment from above, within, and below the LGM section of the core were pre-treated by hydrogen pyrolysis to remove labile carbon from pyrogenic carbon (charcoal) component for radiocarbon dating. The protocol used was identical to that described in Rowe et al. (2019a, 2019b). Pre-treated samples were then combusted to CO_2 and reduced to a graphite target for measurement at ANSTO, as reported in Bird et al. (2014). Age reporting follows Stuiver and Polach (1977), converted into calibrated ages using CALIB REV7.1.0 (Stuiver and Reimer, 1993, Hogg et al., 2013; calibration curve SHCal13). A Bayesian age-depth model was constructed for the LGM interval of core using Bacon 2.2 (Blaauw and Christen, 2011).

RESULTS

Chronology and sedimentology

The depth interval of interest here incorporates two radiocarbon results. However, the overall modelled calibrated chronology is based on four radiocarbon measurements, using samples above and below our interval of interest, from the same core. All sample depths, percent modern carbon (pMC), conventional (yr BP) and calibrated (cal yr BP) radiocarbon ages are listed in Table 1, with the two radiocarbon results pertaining to this study highlighted in grey. The lowermost sample in the interval under consideration in this paper (595 cm) was modelled to ~26,500 cal yr BP, while the uppermost sample at 478 cm was modelled to 18,500 cal yr BP (Fig. 2). The interval thus encompasses a period of 8000 years, with the LGM (21,000 ± 2000 calendar years) represented by samples between 485 cm and 518 cm. The age model in this study differs from that presented in Rowe et al. (2019a) due to subsequent sub-sampling and availability of OZV443 and OZU820 (Table 1).

Sediments are consistent throughout this section of the core, described as dark olive-grey (5Y, 3/2 per Munsell color charts) consolidated and fine clay with decomposed (sapric) organic material. While there is no change in the nature of the sediments in the LGM, sedimentation rate decreases substantially into the LGM (Fig. 2).

Palynological analysis

Sixty pollen taxa were identified in the end-phase last glacial pollen and microcharcoal from Girraween (Fig. 3a, b, c). Unidentified pollen accounted for an average 9% of sample pollen counts. One sample demonstrated low pollen preservation (490 cm, 19.96 cal ka BP) and was excluded from the analysis. Three pollen zones are illustrated; a lower zone labelled GIR-1 (598–524 cm below sediment surface [bss]; ca. 26.53–23.75 cal ka BP), a middle zone labelled GIR-2 (524–493 cm bss; ca. 23.75–20.3 cal ka BP), and an upper zone labelled GIR-3 (493–478 cm bss; ca. 20.3–18.5 cal ka BP).

Zonation was assisted by the numerical classifications. For example, GIR-3 samples have been separated due to very similar values for the three main taxa (Myrtaceae–*Eucalyptus*, Poaceae and Cyperaceae). Zone GIR-1 has been further divided into sub-zones, determined largely by variations in herbaceous pollen (GIR-1a, 598–586 cm bss, ca. 26.53–26.2 cal ka BP; GIR-1b, 586–538 cm bss, ca. 26.2–24.5 cal ka BP; GIR-1c, 538–524 cm bss, ca. 24.5–23.75 cal ka BP). Secondary zonation influences include differences in non-Myrtaceae woody plants. The lower two major zones also show an upward overall decline in charcoal accumulation, crossing over into zone GIR-3 with a sharp increase before decreasing toward the top of the core. A spike in charcoal at 496 cm is the one exception to trends in glacial burning.

https://doi.org/10.1017/qua.2020.50 Published online by Cambridge University Press

Table 1. ^{14}C radiocarbon AMS sample results used to develop the age model presented in Figure 2.

ANSTO code	Submitter ID	Sample Type	Depth (cm)	pMC (%)	^{14}C Age (yr BP)	1σ error (yrs BP)	Calibrated age 95% probability range (cal yr BP)	Calibrated age (median probability)
OZV442	GIR3 E45-50cm	HyPy residue	455	19.9	12,970	80	15,154–17,517	15,692
OZV443	GIR3 F15-20cm	HyPy residue	520	8.62	19,690	90	22,904–24,020	23,568
OZU820	GIR 3 F45cm	HyPy residue	552	6.99	21,370	140	24,306–25,861	25,163
OZU821	GIR 3 G45 cm	HyPy residue	646	5.60	23,160	160	27,272–29,714	27,931

Zone GIR-1 598–524 cm bss, ca. 26.53–23.75 cal ka BP

Zone GIR-1 is dominated by Poaceae (65–82% of the pollen sum), and further characterised by variable total values (and composition) in the minor dryland plant groups, as also reflected in the pollen richness index. Zone GIR-1 contains a high number of Melaleuceae, woody sclerophyll-monsoonal forest taxa (non-eucalypts) and herbaceous pollen types, notably within subzone GIR-1b

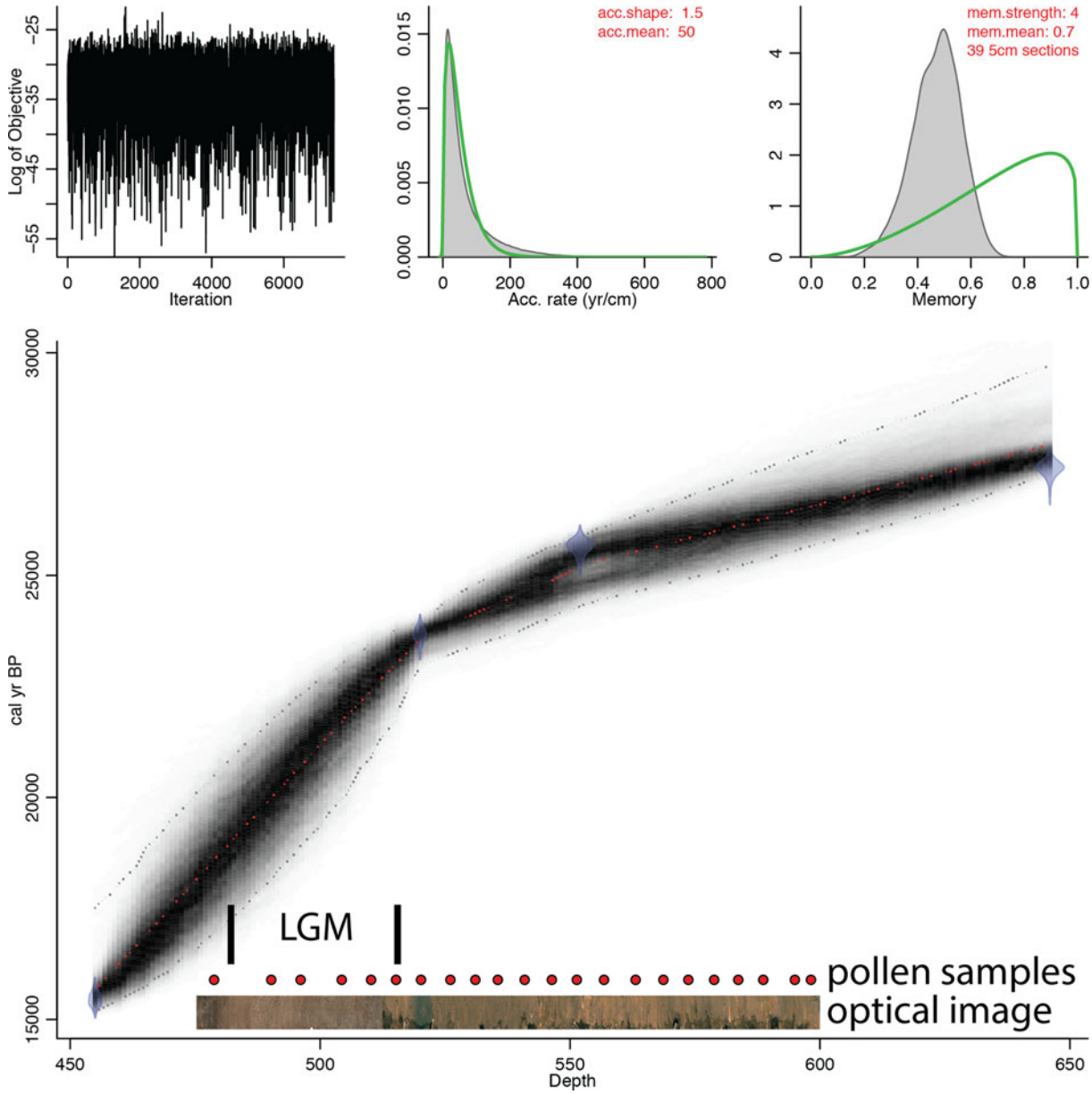

Figure 2. (color online) Age model developed for the interval of core under study. Inset is an optical image of the section from 478 to 595 cm, location of the samples for pollen analysis within the section and interval encompassing the LGM.

https://doi.org/10.1017/qua.2020.50 Published online by Cambridge University Press

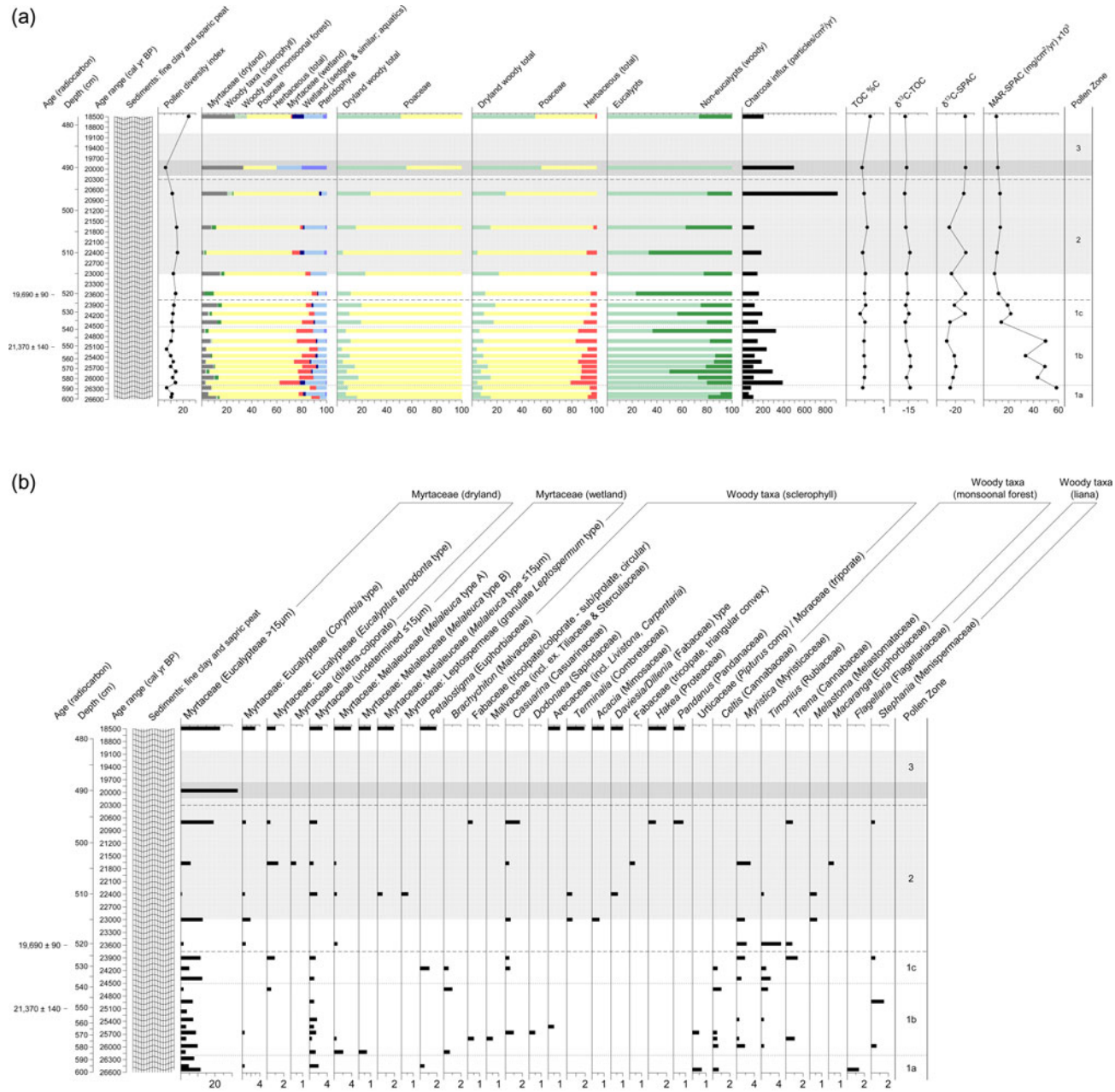

Figure 3. Girraween Lagoon percentage pollen diagram plotted against depth, stratigraphy, radiocarbon results, and calibrated age range. Data presentation divided into: a) pollen group summaries, microcharcoal and geochemical analyses. Note for the $\delta^{13}C$ spectrum we consider -12.5‰ as the cut-off for 100% C_4 grass biomass; b) woody pollen taxa; c) non-woody pollen taxa. The LGM has been highlighted in light grey, with poor pollen sample preservation outlined in darker grey. All percentages derived from total pollen sum including spores. The taxonomic level at which grain identification was most confident is that provided first. All data were plotted using TGView (Grimm, 2004) and pollen assemblages divided into zones based on the stratigraphically constrained classification undertaken by CONISS (Grimm, 1987; 2004). (For interpretation of the references to color in this figure legend, the reader is referred to the web version of this article.)

(26.2–24.5 cal ka BP), after which a number of plants are lost from the record. The representation of minor plant groups and associated diversity decline into subzone GIR-1c (24.5–23.75 cal ka BP), and with relative similarity continuing into zone GIR-2. Upper subzone GIR-1c into zone GIR-2 represents a transitional phase into the LGM.

Larger sized Myrtaceae pollen (grain morphology observed as the eucalypts within the tribe Eucalypteae, see Thornhill et al., 2012; and the author CR's previous Myrtaceae pollen analysis in Stevenson et al., 2015) represent the main tree signal (≤12% of the pollen sum, decreasing to 1.5% at 24.6 cal ka BP) and mixed with sparse sub-canopy tree taxa, including *Brachychiton* and *Casuarina*, and likely

https://doi.org/10.1017/qua.2020.50 Published online by Cambridge University Press

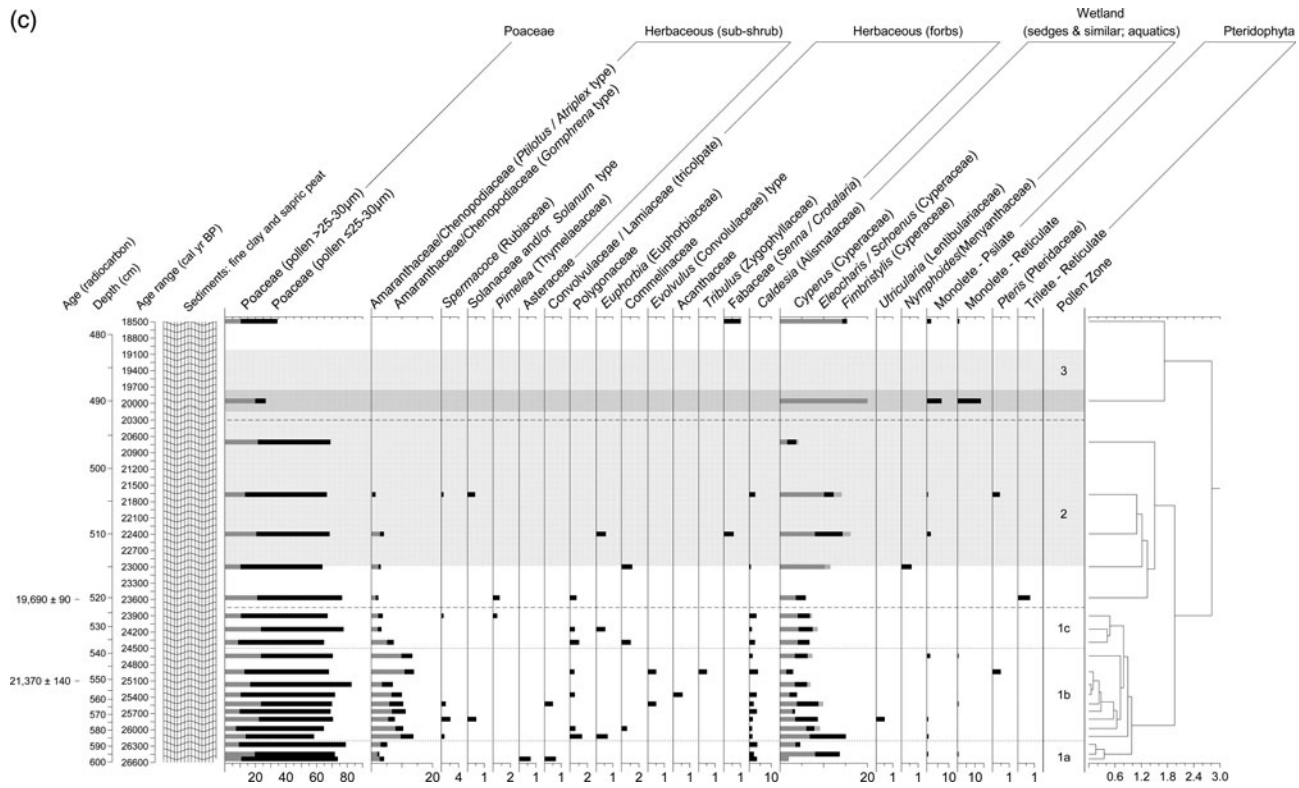

Figure 3. Continued.

shrub types, Malvaceae, Fabcaeae and Arecaceae (all <2%). Monsoonal-forest affiliated Moraceae, *Celtis*, *Timonius*, *Myristica* and *Trema* co-occur in low abundances (also all <2%). Amaranthaceae/Chenopodiaceae (combining *Gomphrena* and *Atriplex-Ptilotus* pollen types) are the major herbaceous taxon (up to 14%), but gradually decline toward zone GIR-2. Other herbs (12 total sub-shrubs and forbs) are sporadic when present.

Zone GIR-1 charcoal records fluctuate, with higher accumulations through subzone GIR-1b (26.2–24.5 cal ka BP). Increases in particles occur at 26.1, 25.8 and 24.6 cal ka BP; greater charcoal coincides with higher and ongoing herbaceous occurrence and expansions in non-eucalypt woody taxa. High zone GIR-1 charcoal is recorded alongside woody (e.g., *Dodonaea*) and herbaceous (e.g., *Euphorbia*) taxa favoured by disturbance, particularly fire (Moore, 2005; Hyland et al., 2010), as well as known open and drier habitat herbaceous 'fire weeds' (e.g., *Solanum*; Moore, 2005).

The Cyperaceae (sedge) family and similarly grouped wetland plants such as *Caldesia* are consistently low (<5% of the pollen sum). No aquatic taxa are recorded. Ferns are occasional, and absent in subzone GIR-1c.

Zone GIR-2 524–493 cm bss, ca. 23.75–20.3 cal ka BP

The bulk of zone GIR-2 encompasses the LGM. Dominant Poaceae pollen percentages continue through this zone (66–76%), and combine with lower proportion, more fluctuating, and less diverse minor plant groups. Woody taxa in all ecological categories show more irregular appearance and abundance than herbaceous plants. When recorded, the eucalypts (0.5–18%) remain the primary sclerophyll tree canopy component, with sub-canopy composition including *Terminalia*, *Acacia*, *Pandanus*, *Hakea* and Fabaceae shrubs such as *Daviesia*. Other members of the Fabaceae family, as well as trees such as *Casuarina*, disappear beginning 20.7 cal ka BP. *Timonius*, *Myristica* and *Trema* remain, and taxa *Melastoma* and Euphorbiaceae-*Macaranga* appear in the record to characterise a monsoonal-forest signal (all <2–4%). No lianas are represented within the forest group. Non-eucalypt pollen outnumbers eucalypt pollen at 23.5 cal ka BP and 22.4 cal ka BP.

As ground cover, Amaranthaceae/Chenopodiaceae types maintain presence (ca. 4%) until 21.6 cal ka BP. Herbs such as *Solanum*, *Euphorbia*, and potential Fabaceae types occur in low abundances, also until 21.6 cal ka BP, after which herbaceous taxa are not recorded until the top of the core. Fern spore values remain low. Wetland elements are similar or slightly higher than in zone GIR-1 and primarily composed of Cyperaceae. Cyperaceae combine with Melaleuceae foremost in the upper part of this zone. A single record of aquatic pollen occurs at 22.4 cal ka BP (*Nymphoides*, <1%).

The scale of zone GIR-2's charcoal accumulation is skewed toward a single peak sample, dated to 20.7 cal ka BP at the top of the zone. Charcoal results are otherwise low and consistent comparative to zone GIR-1.

https://doi.org/10.1017/qua.2020.50 Published online by Cambridge University Press

Zone GIR-3 493–478 cm bss, ca. 20.3–18.5 cal ka BP

The sample at 490 cm depth (age 20 cal ka BP) showed very poor pollen preservation. Vegetation shifts and fire patterns are therefore interpreted with caution. Diversity values are lowest for the record and the majority of plant groups are not recorded. Pollen is dominated by near-even percentages of grass and eucalypts; Cyperaceae (comprising *Cyperus* only) otherwise rise.

The top-most sample (478 cm, 18.5 cal ka BP) is contemporaneous with early-stage deglaciation. Eucalypt values increase from zone GIR-2 (to 22%), and combine with greatest presence (9.5%) sclerophyll sub-canopy woody taxa. Sub-canopy composition is a continuation of that established in zone GIR-2 (*Terminalia*, *Acacia*, *Pandanus*, *Hakea* and Fabaceae shrubs, each at higher individual values), with the reappearance of *Petalostigma* and Arecaceae from before the LGM. Forest associated taxa are absent. Herbaceous, sedge and fern diversity is low. A decline in Poaceae suggests vegetation structure is less open.

Charcoal accumulations progressively decline from the peak observed at 20.7 cal ka BP achieving values similar to the remainder of the record.

Pyrogenic carbon

TOC abundances are uniformly low and relatively constant through the examined interval (from 0.37 to 0.64%, Fig. 3a). PyC mass accumulation rate decreases from 33–58 μg/cm^2/yr before and into the interval identified as the LGM and is relatively stable through and beyond the interval identified as the LGM, with fluxes of 9–22 μg/cm^2/yr. The δ^{13}C values of TOC exhibit a relatively narrow range from -14.7‰ to -16.1‰, indicating a substantial C_4 component, with no overall trend through the interval. The δ^{13}C values of PyC are generally lower than TOC, with a substantially greater range from -14.6‰ to -23.3‰. Overall, there is an irregular trend from lower δ^{13}C values (generally <-20‰) prior to and at the start of the LGM, with higher values (>-20‰) toward the end of the LGM and continuing into the post-glacial period.

DISCUSSION

Vegetation dynamics

Pollen indicates that vegetation characterised by grasses with sparse trees and shrubs occupied Girraween's catchment through the period 26.5–18.5 cal ka BP. While grass communities were the most extensive and continuous pollen-plant group across the area, at no time was the vegetation grass only. This conclusion is supported by high δ^{13}C values in TOC in the sediments throughout the interval under investigation which remain always higher than -16.1‰. This indicates a dominant but not exclusive C_4 (grass) contribution to organic carbon in the sediments. A significant C_4 component also contributed to the PyC preserved in the lake sediment, but δ^{13}C values are lower than for TOC, again indicating that the region was exclusively C_4 (discussed below). Grasses did not extensively co-exist with other ground layer taxa. Although monsoonal-forest taxa (semi-deciduous trees and shrubs, and other tropical elements including Areaceae and lianas) occurred, *Eucalyptus* species (notably *E. tetrodonta*) dominated the tree layer throughout the record, and the woody vegetation was therefore predominantly sclerophyllous. Wetland-associated plants were not widespread landscape components and their presence was determined by localised sinkhole site characteristics.

Preceding the LGM, from 26.6 cal ka BP, grasses were abundant and accompanied by few eucalypts. Vegetation structure showed little sub-canopy layering, with non-eucalypt tree-shrubs sparingly represented and largely consisting of *Petalostigma*. Eucalypts are the only recorded woody taxon at 26.2 cal ka BP. A small range of herbs consisted of Amaranthaceae-Chenopodiaceae types and Asteraceae. After 26.2 cal ka BP the variety of non-eucalypt trees and shrubs (e.g., *Brachychiton, Casuarina*, *Dodonaea*; and monsoonal-forest associated *Celtis*, *Trema* and *Myristica*) increased, but given ongoing high representation of grass pollen, vegetation structure remained very open. Along with Poaceae, understories incorporated a more mixed suite of herbs; foremost after 26.2 cal ka BP Amaranthaceae-Chenopodiaceae (*Ptilotus-Atriplex*, *Gomphrena*) increased, with other herbs (e.g., *Spermacoce*, Polygonaceae, *Evolvulus*) common in various combinations. The herbaceous group may have formed its own small plant associations, as for example within modern inland-arid Australia many forbs are observed to accompany Chenopodiaceae (Moore, 2005).

Transition toward the LGM is evident from 25.3 cal ka BP with the loss of many sub-canopy trees and shrubs, thinning again at 24.9 cal ka BP by the disappearance of numerous minor herbs, and at 24.5 cal ka BP when Amaranthaceae-Chenopodiaceae began to decline. At this same latter time eucalypt presence decreased. Within the formally defined LGM period (21 ± 2 ka BP) the exclusion of herbs is dramatically evident and grasses achieved maximum abundance (22.4 cal ka BP; 77%). Woody components, including eucalypts, fluctuated to an extent not previously seen, and a shift occurred in the composition of sub-canopy non-eucalypts, combining sparse (but more dry adapted, Moore, 2005) *Acacia*, *Terminalia*, *Hakea* and Fabaceae, with declining monsoonal-forest types. This dryland composition, and also fluctuations in these taxa—of eucalypts in particular—was maintained through the deglaciation until the Holocene, at which time mixed woody cover increased to the point of establishing as open forest (Rowe et al., 2019a).

Fire occurred consistently through the entire period, but charcoal particle flux was significantly less than observed during the Holocene (Rowe et al., 2019a), implying comparatively reduced fire activity consistent with significantly lower biomass available to burn. Small increases in fire are evident between 26.2–24.5 cal ka BP, and more dramatically at 20.7 cal ka BP. The PyC fluxes and PyC δ^{13}C values shed

https://doi.org/10.1017/qua.2020.50 Published online by Cambridge University Press

additional light on fire regime through the interval. Unlike the charcoal particle fluxes, PyC flux decreases through GIR zone 1 and remains low in the LGM (GIR zone 2) and immediate post-glacial (GIR zone 3).

Whereas particle counting records all charred particles, not all charred particles will be identified as PyC. Wurster et al. (2013) found almost no PyC was produced by hydrogen pyrolysis at temperatures below ~350°C, with ~50% of charred carbon being identified as PyC by 500°C, and the majority of carbon present as PyC by ~700°C, which was confirmed by McBeath et al. (2015). This implies that the relative difference in trends between particle and PyC fluxes can be interpreted as a relative difference in fire intensity. Thus, fire intensity in GIR Zone 1 (pre-LGM) was initially the highest across the interval examined herein, but declined and stabilized into the LGM. The comparatively high charcoal particle fluxes in upper GIR Zone 2 and lower GIR Zone 3 are not accompanied by increased PyC fluxes, implying relatively low fire intensity. These trends may have been driven simply by declining biomass and fuel connectivity into the LGM. The PyC $\delta^{13}C$ values are lower than TOC $\delta^{13}C$ values, indicating that a substantial fraction of C_4 biomass was completely combusted (or exported as fine aerosol particles) with the char remaining after fires biased toward woody/herbaceous (C_3) particles as has been observed in modern savanna environments (Saiz et al., 2015). PyC $\delta^{13}C$ values do increase irregularly through the entire interval under investigation, implying a slight increase in the proportion of C_4 biomass contributing to the PyC preserved in the record. This is consistent with the slight increase in the proportion of Poaceae pollen (largely at the expense of herbaceous pollen) into the LGM (Figs. 3a, b, c).

Taxon observations

When compared to modern site observations (Schult, 2004), reference pollen data for the NT (Bird et al., 2019), and Holocene ecology (Rowe et al., 2019a, b), Girraween's woody vegetation was less diverse and reduced markedly, but not removed entirely, under glacial conditions. With broad-based estimates of LGM tropical temperatures 3–6°C cooler (Prentice et al., 2017) and weakened hydrological cycles unfavourable for precipitation (Liu, 2018; p. 363) a biogeographic boundary shift occurred across the Darwin region, whereby open xerophytic grassy-savanna similar to that from the NT's continental interior (see Moore, 2005) encroached on a region that is currently mesic-woody-savanna. Key responses at Girraween were high grass representation compared to woody plants, compositional shifts to woody and non-woody dry-adapted taxa, and less plant diversity with restricted wetland affiliates.

Woody biomass and diversity in modern Australian savannas are influenced by water stress (plant available moisture, driven by annual rainfall total and delivery pattern, including dry season length and regularity of storms, Cook et al., 2002; Cook and Heerdegen, 2001). Mapped against declining moisture with distances inland (North Australian Tropical Transect, see also Beringer et al., 2011), Murphy et al. (2015) observe tree loss as well as reduced tree diversity. Hutley et al. (2011) further describe declines in individual tree performance, as measured by stem density, overstorey leaf-area and canopy height. Reduction in these woody structural attributes is interpreted to have occurred alongside site losses of woody taxa through a drier and cooler last glacial at Girraween.

LGM atmospheric CO_2 concentrations were 185 parts-per-million (ppm), compared with 280 ppm pre-industrial values (Schmitt et al., 2012; Calvo and Prentice, 2015). Claussen et al. (2013) emphasise the synergy between last glacial climate and ecophysiological CO_2 impact. In this respect, where glacial climate change influenced NT ecosystem boundaries (plant dispersion), lower CO_2 concentrations invoked C_3-C_4 plant competition, further modifying growth patterns of different plant functional types at Girraween. Prentice and Harrison (2009) highlight low CO_2 individual plant physiological consequences scale up to major ecosystem effects.

At low CO_2 levels, woody C_3 photosynthetic pathways are reduced. In consequence, transpiration and water-use efficiency decrease (Claussen et al., 2013). C_3 plants grown experimentally at low Pleistocene CO_2 levels show strong evidence of stress, including biomass production diminished up to 90% relative to that of plants grown at current atmospheric CO_2. Low CO_2 has also been shown to reduce or prevent reproduction in C_3 species, whereas growth and reproduction of C_4 species (e.g. tropical grasses) are generally unaffected (Ward et al., 2001 and references therein). As a result, there are two explanations for the dominance of C_4 grasses during the last glacial: low CO_2 and drier climate. Grasses would have benefited even further without extensive shading and leaf-litter to negatively affect life-cycle stages such as germination (Scott et al., 2009). Impacts on tree stands include reduced net primary productivity as a result of lower CO_2, enhanced tree-tree competition, and favoured deciduous over evergreen leaf-trait behaviour (Harrison and Prentice, 2003; House et al., 2003).

Between 26.5–18.5 cal ka BP, eucalypts were the main woody taxon through their competitive advantage for water (eucalypts are drought tolerant, Boland et al., 2002, and see Prior, 1997, for *E. tetrodonta*). Eucalypts are also known for high capacities to grow through savanna fire cycles (Murphy et al., 2015). An evergreen monsoonal-forest community at Girraween was unlikely at the last glacial, including at the LGM. Environmental tolerances shown by individual forest-aligned taxa are wider than the forested-type vegetation communities formed by combinations of such taxa (Speck et al., 2010). Abilities to regulate water usage as drought-evading plants (including semi-deciduous, larger seed-size, seed dormancy and/or deep-rooting behaviours; Grubb and Metcalf, 1996; Brock, 2001; Moore, 2005; Jeremy Russell-Smith and Setterfield, 2006), helps explains the presence of *Timonius*, *Celtis*, *Trema*, Moraceae (e.g., *Ficus*), Areaceae (e.g., *Livisonta*), and *Macaranga*, as well as *Terminalia* and *Brachychiton*. It positions them as intermediate taxa within

https://doi.org/10.1017/qua.2020.50 Published online by Cambridge University Press

the eucalypts at Girraween (cf. Speck et al., 2010). While water scarcity by itself appears unlikely to have been critical for forest taxa tolerant of drought, it (in combination with low CO_2) likely rendered them inferior eucalypt competitors (Murphy et al., 2015; House et al., 2003). Vulnerability to fire may also have been enhanced (see below; Brock, 2001).

Woody taxa are rarely continuously maintained for more than one sample (Fig. 3b). This data pattern continues into the early stages of the Holocene (Rowe et al., 2019a, and Figs. 2b and c), and variations in pollen counts are acknowledged as much as actual variation in plant abundance. The speculation here is that plants are capable of episodic growth responses following potential periodic monsoon-moisture availability, but do not demonstrate long-term recovery and expansion suggestive of an overall long-term unfavourable climate. Rapid responses, as well as short-lived taxa such as *Macaranga* and Fabaceae types are indicative of an overall increase in ecosystem turnover rates under the influence of glacial to post-glacial to early Holocene conditions (cf. Haberle, 2005). The extent of glacial climatic and low CO_2 driven woody suppression is also evident, where low fire frequency is otherwise associated with tree-shrub recruitment (canopy and/or sub-canopy development, Scholes and Archer, 1997; Scott et al., 2009). Taking further cues from the modern NT interior (see above; Moore 2005; Hutley et al., 2011), at Girraween woody plants may have occurred as scattered individuals above the grasses. Mixed composition discrete woody vegetation structures potentially existed as fragments of woodland which persisted from earlier periods of more favourable climate within habitat pockets. Grouping of woody plants may also have developed in relation to fire events.

The combined effect of relatively lower glacial precipitation, cool temperatures, low CO_2, and lower biomass of sclerophyll woodland would have been sufficient to dramatically reduce charcoal deposition. Comparison with Rowe et al. (2019a) and Bird et al. (2019) suggests Girraween had a lower capacity to carry fire, and was subject to a relatively uniform fire regime during the LGM. Savanna studies refer to fire as a top-down factor influencing grass-woody layer compositions as opposed to bottom-up environmental factors such as plant-available moisture and edaphic properties (Scholes and Archer, 1997; Scott et al., 2009). The results of this study suggest top-down fire processes played less of a role in the LGM in determining vegetation than in the Holocene and modern day. Grasses in the LGM were little affected by burning; eucalypts were also unresponsive. Fire appears to have exerted only selective influence on minor woody plant groups such as the non-eucalypts and herbs. As one theory, low-level fire potentially assisted to release nutrients into an overall nutrient deficient savanna ecosystem (Richards et al., 2011; Cook, 1994), to benefit restricted and/or lesser-drought-tolerant taxa. The germination of herbs can also be favoured by heat and smoke after burning, and fire can promote flowering (Fensham et al., 2002; Nano and Clarke, 2011; and under less intense fire as defined by Richards et al., 2011, p. 504).

We conclude that glacial climate change and CO_2 effects were primary factors dictating Girraween's vegetation structure and composition, and were also the primary factors influencing fire in the region. Site characteristics were a secondary determinant. The sinkhole depression would vary in microclimate, soil types, water drainage, and potentially be less exposed to fire than the wider landscape, thereby providing a major source of pocket habitats for plants. This would have been the primary influence on the presence and distribution of wetland plant assemblages during the end-stage glacial and LGM, and the location from which wetland plants expand during deglaciation. Taxa such as *Melaleuca*, Cyperaceae (*Cyperus*, *Eleocharis*/*Schoenus*, *Fimbristylis*), *Caldesia* and the Pteridophyta were more likely to be located within the depression adjacent to the sinkhole than to occupy the open grassy catchment. The surrounding catchment was a drier, more exposed, and more uniform habitat. This limited wetland-related flora, which was unable to effectively compete with dry-resisting or dry-evading taxa, woody and non-woody alike. Any plant within the sinkhole would in turn provide a surface-stabilising effect, generally capable of protecting depression slopes from erosion. The sinkhole waterbody did not support an aquatic plant community. Glacial stage drawdowns likely affected aquatic plants directly through exposure to aerial conditions and indirectly through substrate modification. Droughts and/or limited water exchange can produce anoxic (reducing) conditions that are toxic to many water plants (Santamaria, 2002; Bornette and Puijalon, 2011). As per slow decomposition of dryland soil organic matter, cooler water temperatures also slow down the mineralisation of organic matter, impeding nutrient release into the water column for taxa such as *Nymphaea* (Bornette and Puijalon, 2011).

Climate inferences

The palynological results presented here along with an understanding of the coastline position at the LGM enable a semi-quantitative estimate of annual rainfall at Girraween Lagoon during the LGM. The coastline was approximately 300 km north and northwest of the site during the LGM (Ishiwa et al., 2019). Assuming no diminution of monsoon intensity and applying the modern continental rainfall gradient would imply that rainfall was diminished from 1700 mm to approximately 1000 mm (Cook and Heerdegen, 2001). Also by analogy with modern climate in the region, seasonality would be increased with duration of the rainy season decreased from 200 days to 150 days (Cook and Heerdegen, 2001).

E. tetrodonta pollen is not common but remains represented in LGM samples (Fig. 3b). This species is relatively common in regions with ~700 mm annual rainfall (Boland et al., 2006) with exceptional occurrences down to 500 mm. This does not take into account the effect of either decreased CO_2 or temperature during the LGM on species distribution, however these changes act in opposite directions on vegetation. Decreased CO_2 is likely to have decreased the competitiveness of woody C_3 biomass compared to grass-dominated C_4 biomass

https://doi.org/10.1017/qua.2020.50 Published online by Cambridge University Press

Figure 4. (color online) Representation of LGM vegetation based on the conclusion of decreased mean annual rainfall at Girraween Lagoon to within 700–1000 mm (annual precipitation derived from the general lower range for *Eucalyptus tetrodonta*, and the precipitation implied by moving 300 km inland from Darwin today). Reduction in tree cover and stature, loss of woody-plant richness and expansion of grassland relative to current vegetation at the site: *left*, Girraween Lagoon, August 2018, and *right*, Jindare Station, September 2015, located within the Northern Territory's 1000 mm isohyet and illustrative of the upper range and conditions at Girraween during the last glacial phase.

(Prentice et al., 2017). Decreased LGM temperature, the magnitude of which is poorly constrained in the study region (e.g., Cleator et al., 2019) would decrease evaporation and therefore increase effective plant available moisture for a given mean annual rainfall (Liu et al., 2018). By combining coastline position and *E. tetrodonta* rainfall requirements we thus conclude that mean annual rainfall at Girraween Lagoon was most likely in the range 700–1000 mm (Fig. 4).

Our results are generally consistent with recent modelling results for the LGM globally (Jiang et al., 2015) and for the northern Australian region (Yan et al., 2018). These studies indicate that there was still an effective monsoon rainfall regime across the northern Australian region, in accordance with earlier studies (e.g. Marshall and Lynch, 2008). Yan et al. (2018) conclude that changes in land-sea distribution and east-west gradients in sea surface temperature resulted in a modest lowering of total rainfall but an increase in rainfall seasonality across northern Australia, again in accord with previous studies (Marshall and Lynch, 2008). These results suggest that a value towards the lower rainfall boundary suggested above is more likely than the upper rainfall boundary and that the monsoon season duration of 150 days inferred above is more likely an upper boundary.

Jiang et al. (2015) specifically note a lack of correspondence between their modelling results and conclusions based on (very sparse) northern Australian climate proxy records for the LGM. This appears to largely be an artefact of terminology. The LGM coastline was between 200 and 500 km seaward of the modern coastline along the entire length of western northern Australia (Fig. 1), and this means that the change in coastline position will have dramatically decreased precipitation at any terrestrial site simply due to the strong rainfall gradient into the interior. A corollary of this is that monsoon rainfall may not have penetrated far into south-draining catchments, and hence low lake levels are recorded in the arid northern Australian interior at the LGM (e.g., Fitzsimmons et al., 2012). So while the modern Australian terrestrial region was more arid at the LGM, this does not imply monsoon failure, but more likely a shift of the majority of monsoon rainfall onto the now-flooded continental shelf. Palynological investigation of deep sea cores between Australia and New Guinea, which therefore were exposed to pollen rain from the exposed continental shelf of Australia, do show an expansion of grassland at the LGM (e.g., van der Kaars, 1991). This suggests that some combination of rainfall amount, seasonality, reduced CO_2 and reduced temperature did lead to a general reduction in tree cover over that expected simply from the operation of a continental rainfall gradient similar to that currently observed.

CONCLUSIONS

Girraween Lagoon remained a perennial water body throughout the LGM and as a result retains a proxy record of the LGM environment. The palynological results for the LGM interval indicate a dramatic reduction in tree cover and expansion of grassland relative to current tall woodland vegetation at the site. Dryland vegetation during the LGM interval is best described as an open xerophytic grassy-savanna. In terms of the megabiome classification of Dallmeyer et al. (2019), the site is likely on the boundary between grassland/dry shrubland and savanna/dry woodland. In other DGVM classification schemes the Girraween site is best characterized as close to the boundary of plant functional types variously described as grassland, xerophytic shrubland, grassland/shrubland, and tropical savanna (e.g., Calvo and Prentice, 2015).

No inference can be drawn with respect to LGM temperature at the site, but rainfall may be constrained to 700–1000 mm,

https://doi.org/10.1017/qua.2020.50 Published online by Cambridge University Press

more likely toward the lower than the upper bound, and wet season length was likely <150 days. The monsoon remained active but most monsoon rainfall fell on the now-flooded continental shelf as a result of a steep rainfall gradient into the continental interior, similar to that which pertains today.

Girraween Lagoon and other permanent water bodies in the Darwin region would have enabled continued human occupation of the area through the LGM, although there is currently no dated evidence of human activity in the region at that time.

ACKNOWLEDGMENTS

This research was funded by the Australian Research Council Centre of Excellence for Australian Biodiversity and Heritage (CE170100015) and an Australian Research Council Laureate Fellowship to M.I.B. (FL140100044). L.H. is recipient of Discovery Project DP130100334. V.L. acknowledges the financial support from the Australian Government for the Centre for Accelerator Science at ANSTO, where the measurements were done, through the National Collaborative Research Infrastructure Strategy (NCRIS), and expresses gratitude to the radiocarbon laboratory staff who processed our samples. Rainy Comley's assistance within the JCU laboratories was greatly appreciated. Warm thanks to the Larrakia Nation, Larrakia Ranger group, and the wider Larrakia community for their support and local insights into the Girraween environment. Access assistance from Graham Churcher is also gratefully acknowledged. Thanks also to Ron Innes for engineering work on the raft and coring equipment. The authors also appreciate the feedback provided by two reviews on earlier drafts.

REFERENCES

Alder, J.R., Hostetler, S.W., 2015. Global climate simulations at 3000-year intervals for the last 21000 years with the GENMOM coupled atmosphere-ocean model. *Climate of the Past* 11, 449–471.

Ascough, P.L., Bird, M.I., Brock, F., Higham, T.F.G., Meredith, W., Snape, C.E., Vane, C.H., 2009. Hydropyrolysis as a new tool for radiocarbon pre-treatment and the quantification of black carbon. *Quaternary Geochronology* 4, 140–147.

Bartlein, P.J., Harrison, S.P., Brewer, S., Connor, S., Davis, B.A.S., Gajewski, K., Guiot, J., Harrison-Prentice, T.I., Henderson, A., Peyron, O. and Prentice, I.C., 2011. Pollen-based continental climate reconstructions at 6 and 21 ka: a global synthesis. *Climate Dynamics,* 37, 775–802.

Beringer, J., Hutley, L.B., Hacker, J.M., Neininger, B. 2011. Patterns and processes of carbon, water and energy cycles across northern Australian landscapes: from point to region. *Agricultural and Forest Meteorology* 151, 1409–1416.

Bird, M.I., Brand, M., Diefendorf, A.F., Haig, J.L., Hutley, L.B., Levchenko, V., Ridd, P.V., *et al*.., 2019. Identifying the 'savanna' signature in lacustrine sediments in northern Australia. *Quaternary Science Reviews* 203, 233–247.

Bird, M.I., Levchenko, V., Ascough, P.L., Meredith, W., Wurster, C.M., Williams, A., Tilston, E.L., Snape, C.E. and Apperley, D.C., 2014. The efficiency of charcoal decontamination for radiocarbon dating by three pre-treatments–ABOX, ABA and hypy. *Quaternary Geochronology,* 22, 25–32.

Blaauw, M., and Christen, J.A., 2011. Flexible paleoclimate age-depth models using an autoregressive gamma process. *Bayesian analysis* 6, 457–474.

Blonder, B., Enquist, B.J., Graae, B.J., Kattge, J., Maitner, B.S., Morueta-Holme, N., Ordonez, A., *et al*.., 2018. Late Quaternary climate legacies in contemporary plant functional composition. *Global Change Biology* 24, 4827–4840.

Boland, D.J., Brooker, M.I.H., Chippendale, G.M., Hall, N., Hyland, B.P.M., Johnston, R.D., Kleinig, D.A., McDonald, M.W., Turner, J.D. 2006. *Forest trees of Australia*. CSIRO Publishing, Melbourne.

Bornette, G., Puijalon, S., 2011. Response of aquatic plants to abiotic factors: a review. *Aquatic Sciences* 73, 1–14.

Brock, J., 1995. Remnant Vegetation Survey Darwin to Palmerston Region. A Report to Greening Australia, Darwin, Northern Territory.

Brock, J., 2001. *Native plants of northern Australia*. Reed New Holland, Sydney.

Bureau of Meteorology (BoM), 2019. Weather and Climate Data. Commonwealth of Australia. http://www.bom.gov.au/climate/data/ (Accessed August 2019).

Burns, T., 1999. Subsistence and settlement patterns in the Darwin coastal region during the late Holocene: a preliminary report of archaeological research. *Australian Aboriginal Studies* 1, 59–69.

Calvo, M.M.and Prentice, I.C., 2015. Effects of fire and CO 2 on biogeography and primary production in glacial and modern climates. *New Phytologist* 208, 987–994.

Charles, S., Petheram, C., Berthet, A., Browning, G., Hodgson, G., Wheeler, M., Yang, A., *et al*., 2016. Climate data and their characterisation for hydrological and agricultural scenario modelling across the Fitzroy, Darwin and Mitchell catchments: a technical report to the Australian Government from the CSIRO Northern Australia Water Resource Assessment, part of the National Water Infrastructure Development Fund: Water Resource Assessments. CSIRO, Australia.

Chen, W., Zhu, D., Ciais, P., Huang, C., Viovy, N., Kageyama, M., 2019. Response of vegetation cover to CO2 and climate changes between last glacial maximum and pre-industrial period in a dynamic global vegetation model. *Quaternary Science Reviews* 218, 293–305.

Clark, P.U., Dyke, A.S., Shakun, J.D., Carlson, A.E., Clark, J., Wohlfarth, B., Mitrovica, J.X., Hostetler, S.W. and McCabe, A.M., 2009. The last glacial maximum. *Science,* 325, 710–714.

Claussen, M., Selent, K., Brovkin, V., Raddatz, T., Gayler, V., 2013. Impact of CO2 and climate on last glacial maximum vegetation—a factor separation. *Biogeosciences* 10, 3593–3604.

Cleator, S., Harrison, S.P., Nichols, N., Prentice, I.C., Roulstone, I., 2019. A new multi-variable benchmark for last glacial maximum climate simulations. University of Reading. Dataset. DOI, 10 (1947.206).

Cook, G.D., 1994. The fate of nutrients during fires in a tropical savanna. *Australian Journal of Ecology* 19, 359–365.

Cook, G.D., Heerdegen, R.G., 2001. Spatial variation in the duration of the rainy season in monsoonal Australia. *International Journal of Climatology: A Journal of the Royal Meteorological Society* 21, 1723–1732.

Cook, G.D., Williams, R.J., Hutley, L.B., O'Grady, A.P. and Liedloff, A.C., 2002. Variation in vegetative water use in the savannas of the North Australian Tropical Transect. *Journal of Vegetation Science* 13, 413–418.

Dallmeyer, A., Claussen, M., Brovkin, V., 2019. Harmonising plant functional type distributions for evaluating earth system models. *Climate of the Past* 15, 335–366.

https://doi.org/10.1017/qua.2020.50 Published online by Cambridge University Press

Denniston, R.F., Asmerom, Y., Polyak, V.J., Wanamaker Jr, A.D., Ummenhofer, C.C., Humphreys, W.F., Cugley, J., Woods, D., Lucker, S., 2017. Decoupling of monsoon activity across the northern and southern Indo-Pacific during the late glacial. *Quaternary Science Reviews* 176, 101–105.

Fensham, R.J., Fairfax, R.J., Holman, J.E., 2002. Response of a rare herb (*Trioncinia retroflexa*) from semi-arid tropical grassland to occasional fire and grazing. *Austral Ecology* 27, 284–290.

Fitzsimmons, K.E., Miller, G.H., Spooner, N.A., Magee, J.W., 2012. Aridity in the monsoon zone as indicated by desert dune formation in the Gregory Lakes basin, northwestern Australia. *Australian Journal of Earth Sciences* 59, 469–478.

Ganopolski, A., Rahmstorf, S., Petoukhov, V., Claussen, M., 1998. Simulation of modern and glacial climates with a coupled global model of intermediate complexity. *Nature* 391, 351–356.

Gavashelishvili, A., Tarkhnishvili, D., 2016. Biomes and human distribution during the last ice age. *Global Ecology and Biogeography* 25, 563–574.

Grimm, E.C., 1987. CONISS: a FORTRAN 77 program for stratigraphically constrained cluster analysis by the method of incremental sum of squares. *Computers and Geosciences* 13, 13–35

Grimm, E.C., 2004. Tilia graph v. 2.0.2. Illinois State Museum, Research and Collections Center.

Grubb, P.J., Metcalfe, D.J., 1996. Adaptation and inertia in the Australian tropical lowland rain-forest flora: contradictory trends in intergeneric and intrageneric comparisons of seed size in relation to light demand. *Functional Ecology* 10, 512–520.

Haberle, S.G., 2005. A 23,000-yr pollen record from Lake Euramoo, wet tropics of NE Queensland, Australia. *Quaternary Research* 64, 343–356.

Harrison, S.P., Bartlein, P.J., Izumi, K., Li, G., Annan, J., Hargreaves, J., Braconnot, P., Kageyama, M., 2015. Evaluation of CMIP5 palaeo-simulations to improve climate projections. *Nature Climate Change,* 5, 735–743.

Harrison, S.P., Prentice, C.I., 2003. Climate and CO2 controls on global vegetation distribution at the last glacial maximum: analysis based on palaeovegetation data, biome modelling and palaeoclimate simulations. *Global Change Biology* 9, 983–1004.

Hogg, A.G., Hua, Q., Blackwell, P.G., Niu, M., Buck, C.E., Guilderson, T.P., Heaton, T.J., Palmer, J.G., Reimer, P.J., Reimer, R.W. and Turney, C.S., 2013. SHCal13 Southern Hemisphere calibration, 0–50,000 year cal BP. *Radiocarbon* 55, 1889–1903.

Hopcroft, P.O., Valdes, P.J., 2015. How well do simulated last glacial maximum tropical temperatures constrain equilibrium climate sensitivity? *Geophysical Research Letters* 42, 5533–5539.

House, J.I., Archer, S., Breshears, D.D., Scholes, R.J., 2003. Conundrums in mixed woody–herbaceous plant systems. *Journal of Biogeography* 30, 1763–1777.

Hutley, L.B., Beringer, J., Isaac, P.R., Hacker, J.M., Cernusak, L.A., 2011. A sub-continental scale living laboratory: spatial patterns of savanna vegetation over a rainfall gradient in northern Australia. *Agricultural and Forest Meteorology* 151, 1417–1428.

Hutley L.B., Evans B.J., Beringer J., Cook G.D., Maier S.W., Razon, E., 2013. Impacts of an extreme cyclone event on landscape-scale savanna fire, productivity and greenhouse gas emissions. *Environmental Research Letters* 8, 1–12.

Hyland, B.P.M., Whiffin, T., and Zich, F.A., 2010. *Australian Tropical Rainforest Plants*. CSIRO Plant Industry and Centre for Australian National Biodiversity Research, Canberra.

Ishiwa, T., Yokoyama, Y., Okuno, J.I., Obrochta, S., Uehara, K., Ikehara, M., Miyairi, Y., 2019. A sea-level plateau preceding the Marine Isotope Stage 2 minima revealed by Australian sediments. *Scientific Reports* 9, 6449.

Jiang, D., Tian, Z., Lang, X., Kageyama, M., Ramstein, G., 2015. The concept of global monsoon applied to the last glacial maximum: a multi-model analysis. *Quaternary Science Reviews* 126, 126–139.

Liu, S., Jiang, D., Lang, X., 2018. A multi-model analysis of moisture changes during the last glacial maximum. *Quaternary Science Reviews* 191, 363–377.

Lu, Z., Miller, P.A., Zhang, Q., Wårlind, D., Nieradzik, L., Sjolte, J., Li, Q., Smith, B., 2019. Vegetation pattern and terrestrial carbon variation in past warm and cold climates. *Geophysical Research Letters* 8133–8143.

Marshall, A.G., Lynch, A.H., 2008. The sensitivity of the Australian summer monsoon to climate forcing during the late Quaternary. *Journal of Geophysical Research: Atmospheres*, 113(D11).

McBeath, A.V., Wurster, C.M., Bird, M.I., 2015. Influence of feedstock properties and pyrolysis conditions on biochar carbon stability as determined by hydrogen pyrolysis. *Biomass and Bioenergy* 73, 155–173.

McFarlane, M.J., Ringrose, S., Giusti, L., Shaw, P.A., 1995. The origin and age of karstic depressions in the Darwin-Koolpinyah area of the Northern Territory of Australia. In: Brown (Ed.), *Geomorphology and Groundwater*. John Wiley and Sons Limited, Chichester, United Kingdom.

Meredith, W., Ascough, P.L., Bird, M.I., Large, D.J., Snape, C.E., Sun, Y., Tilston, E.L. 2012. Assessment of hydropyrolysis as a method for the quantification of black carbon using standard reference materials. *Geochimica et Cosmochimica Acta* 97, 131–147.

Moore C.E., Beringer J., Evans B., Hutley L.B., McHugh I., Tapper N.J., 2016. The contribution of trees and grasses to productivity of an Australian tropical savanna. *Biogeosciences* 13, 2387–2403.

Moore, P., 2005. *Plants of inland Australia*. Reed New Holland, Sydney.

Murphy B.P., Liedloff A.C., Cook, G.D., 2015. Does fire limit tree biomass in Australian savannas? *International Journal of Wildland Fire* 24, 1–13.

Nano, C.E., Clarke, P.J., 2011. How do drought and fire influence the patterns of resprouting in Australian deserts? *Plant Ecology*, 212, 2095–2110.

Peel, M.C., Finlayson, B.L., and McMahon, T.A., 2007. Updated world map of the Köppen-Geiger climate classification. *Hydrology and earth system sciences discussions* 4, 439–473.

Pickett, E.J., Harrison, S.P., Hope, G., Harle, K., Dodson, J.R., Peter Kershaw, A., Colin Prentice, I., *et al*., 2004. Pollen-based reconstructions of biome distributions for Australia, Southeast Asia and the Pacific (SEAPAC region) at 0, 6000 and 18,000 ^{14}C yr BP. *Journal of Biogeography* 31, 1381–1444.

Prentice, I.C., Cleator, S.F., Huang, Y.H., Harrison, S.P. Roulstone, I., 2017. Reconstructing ice-age palaeoclimates: quantifying low-CO2 effects on plants. *Global and Planetary Change* 149, 166–176.

Prentice, I.C., Cramer, W., Harrison, S.P., Leemans, R., Monserud, R.A., Solomon, A.M., 1992. Special paper: a global biome model based on plant physiology and dominance, soil properties and climate. *Journal of Biogeography* 19, 117–134.

Prentice, I.C., Harrison, S.P., 2009. Ecosystem effects of CO2 concentration: evidence from past climates. *Climate of the Past* 5, 297–307.

Prior, L.D., 1997. *Ecological Physiology of* Eucalyptus tetrodonta *(F. Muell.) and T*erminalia ferdinandiana *(Excell.) Saplings in the Northern Territory*. Unpublished PhD thesis. Charles Darwin University, Northern Territory, Australi

https://doi.org/10.1017/qua.2020.50 Published online by Cambridge University Press

Richards, A.E., Cook, G.D., Lynch, B.T., 2011. Optimal fire regimes for soil carbon storage in tropical savannas of northern Australia. *Ecosystems* 14, 503–518.

Rowe, C., Brand, M., Hutley, L.B., Wurster, C., Zwart, C., Levchenko, V., Bird, M., 2019a. Holocene savanna dynamics in the seasonal tropics of northern Australia. *Review of Palaeobotany and Palynology* 267, 17–31.

Rowe, C., Brand, M., Hutley, L.B., Zwart, C., Wurster, C., Levchenko, V., Bird, M., 2019b. Understanding Australian tropical savanna: environmental history from a pollen perspective. *Northern Territory Naturalist* 29, 2–11.

Russell-Smith, J., Setterfield, S.A., 2006. Monsoon rain forest seedling dynamics, northern Australia: contrasts with regeneration in eucalypt-dominated savannas. *Journal of Biogeography* 33, 1597–1614.

Russell-Smith, J. and Yates, C.P., 2007. Australian savanna fire regimes: context, scales, patchiness. *Fire ecology*, 3, pp.48–63.

Saiz, G., Wynn, J.G., Wurster, C.M., Goodrick, I., Nelson, P.N., Bird, M.I., 2015. Pyrogenic carbon from tropical savanna burning: production and stable isotope composition. *Biogeosciences* 12, 1849–1863.

Santamaría, L., 2002. Why most aquatic plants are widely distributed: dispersal, clonal growth and small-scale heterogeneity in a stressful environment. *Actaoecologica* 23, 137–154.

Scheiter, S., Higgins, S.I., Beringer, J., Hutley, L.B., 2015. Climate change and long-term fire management impacts on Australian savannas. *New Phytologist* 205, 1211–1226.

Schmitt, J., Schneider, R., Elsig, J., Leuenberger, D., Lourantou, A., Chappellaz, J., Kohler, P., *et al*., 2012. Carbon isotope constraints on the deglacial CO_2 rise from ice cores. *Science* 336, 711–714.

Scholes, R.J., Archer, S.R., 1997. Tree-grass interactions in savannas. *Annual Review of Ecological Systematics* 28, 517–544.

Schult, J., 2004. An Inventory of the Freshwater Lagoons in the Darwin Region. Report No. 36/2004D, Water Monitoring Branch, Department of Infrastructure, Planning and Environment, Palmerston, Northern Territory.

Scott, K.A., Setterfield, S.A., Andersen, A.N., Douglas, M.M., 2009. Correlates of grass-species composition in a savanna woodland in northern Australia. *Australian Journal of Botany* 57, 10–17.

Shakun, J.D., Carlson, A.E., 2010. A global perspective on last glacial maximum to Holocene climate change. *Quaternary Science Reviews* 29, 1801–1816.

Speck, N.H., Wright, R.L., Stewart, G.A., Fitzpatrick, E.A., Mabbutt, J.A., van de Graaf, R.H.M., 2010. General Report on Lands of the Tipperary Area, Northern Territory, 1961. *CSIRO Land Research Surveys,* 13, 1–118.

Stevenson, J., Brockwell, S., Rowe, C., Proske, U., Shiner, J., 2015. The palaeo-environmental history of Big Willum Swamp, Weipa: an environmental context for the archaeological record. *Australian Archaeology* 80, 17–31.

Stuiver, M., and Polach, H.A., 1977. Reporting of C-14 data-Discussion. *Radiocarbon* 19, 355–363.

Stuiver, M., and Reimer, P.J., 1993. Extended 14C data base and revised CALIB 3.0 14 C age calibration program. *Radiocarbon* 35, 215–230.

Thornhill, A.H., Hope, G.S., Craven, L.A., Crisp, M.D., 2012. Pollen morphology of the Myrtaceae. Part 1: tribes Eucalypteae, Lophostemoneae, Syncarpieae, Xanthostemoneae and subfamily Psiloxyloideae. *Australian Journal of Botany* 60, 65–199.

Vahdati, A.R., Weissmann, J.D., Timmermann, A., de León, M.S.P., Zollikofer, C.P., 2019. Drivers of late Pleistocene human survival and dispersal: an agent-based modeling and machine learning approach. *Quaternary Science Reviews* 221, 105867.

Van der Kaars, W.A., 1991. Palynology of eastern Indonesian marine piston-cores: a late Quaternary vegetational and climatic record for Australasia. *Palaeogeography, Palaeoclimatology, Palaeoecology* 85, 239–302.

Ward, J.K., Tissue, D.T., Thomas, R.B., Strain, B.R., 2001. Comparative responses of model C_3 and C_4 plants to drought in low and elevated CO2. *Global Change Biology* 5, 857–867.

Webb, L.J. and Tracey, J.G. 1994. The rainforests of northern Australia. In, Groves, R.H. (Ed.) *Australian Vegetation*. Cambridge University Press, Cambridge, UK, pp 87–130.

Weigelt, P., Steinbauer, M.J., Cabral, J.S., Kreft, H., 2016. Late Quaternary climate change shapes island biodiversity. *Nature* 532, 99–102.

Wells, S., 2001. *Saltwater people: Larrakia stories from around Darwin*. Larrakia Nation Aboriginal Corporation, Darwin, Northern Territory.

Whitlock, C., Larsen, C., 2002. Charcoal as a fire proxy. In: Smol, J.P., Birks, H.J.B., Last, W., Bradley, R.S., Alverson, K. (Eds.) *Tracking Environmental Change Using Lake Sediments*. Springer Publishing, Netherlands, pp. 75–97.

Williams, A.N., Ulm, S., Sapienza, T., Lewis, S., Turney, C.S., 2018. Sea-level change and demography during the last glacial termination and early Holocene across the Australian continent. *Quaternary Science Reviews* 182, 144–154.

Wurster, C.M., Lloyd, J., Goodrick, I., Saiz, G., Bird, M.I., 2012. Quantifying the abundance and stable isotope composition of pyrogenic carbon using hydrogen pyrolysis. *Rapid Communications in Mass Spectrometry* 26, 2690–2696.

Wurster, C.M., Saiz, G., Schneider, M.P.W., Schmidt, M.W.I., Bird, M.I., 2013. Quantifying pyrogenic carbon from thermosequences of wood and grass using hydrogen pyrolysis. *Organic Geochemistry* 62, 28–32.

Yan, M., Wang, B., Liu, J., Zhu, A., Ning, L., Cao, J., 2018. Understanding the Australian monsoon change during the last glacial maximum with a multi-model ensemble. *Climate of the Past* 14, 2037–2052.

Ye, J.S., Delgado-Baquerizo, M., Soliveres, S., Maestre, F.T., 2019. Multifunctionality debt in global drylands linked to past biome and climate. *Global Change Biology* 25, 2152–2161.

Yokoyama, Y., Hirabayashi, S., Goto, K., Okuno, J.I., Sproson, A.D., Haraguchi, T., Ratnayake, N. and Miyairi, Y., 2019. Holocene Indian Ocean sea level, Antarctic melting history and past Tsunami deposits inferred using sea level reconstructions from the Sri Lankan, Southeastern Indian and Maldivian coasts. *Quaternary Science Reviews,* 206, 150–161.

Zhu, D., Ciais, P., Chang, J., Krinner, G., Peng, S., Viovy, N., Peñuelas, J., Zimov, S., 2018. The large mean body size of mammalian herbivores explains the productivity paradox during the last glacial maximum. *Nature Ecology and Evolution* 2, 640–649.

https://doi.org/10.1017/qua.2020.50 Published online by Cambridge University Press